

Alteration of Coenzyme Specificity of Malate Dehydrogenase from *Thermus flavus* by Site-directed Mutagenesis*

(Received for publication, October 9, 1992)

Makoto Nishiyama‡§, Jens J. Birktoft¶, and Teruhiko Beppu§

From the §Department of Agricultural Chemistry, Faculty of Agriculture, The University of Tokyo, Tokyo 113, Japan and the ¶Department of Biochemistry and Molecular Biophysics, Washington University School of Medicine, St. Louis, Missouri 63110

On the basis of the crystal structure of the NAD-dependent cytoplasmic malate dehydrogenase (MDH) and its alignment with NADP-dependent counterparts, the loop region between β -strand B and α -helix C in the dinucleotide-binding fold was predicted as a principal determinant for the coenzyme specificity. Two mutants, EX7 and EX3, of NAD-dependent MDH from *Thermus flavus* were constructed. In the EX7 mutant, the seven loop amino acids in positions 41–47, Glu-Ile-Pro-Gln-Ala-Met-Lys, were replaced by the corresponding loop residues in the NADP-dependent MDH from chloroplasts, Gly-Ser-Glu-Arg-Ser-Phe-Gln. In the EX3 mutant, Glu-41, Ile-42, and Ala-45 were substituted with the corresponding 3 amino acids in the NADP-dependent chloroplast MDH. In both mutations the coenzyme specificity was altered from NAD to NADP. Especially, the EX7 mutation resulted in a more than 1000-fold improvement in overall catalytic efficiency with NADPH and a 600-fold decrease in the efficiency with NADH as cofactors. Consequently, EX7 mutant was 132 times more efficient with NADPH than NADH without a large decrease in turnover number.

The NADP-dependent malate dehydrogenases (EC 1.1.1.82) from chloroplasts (chMDH)¹ (1–3) displays a significant identity in amino acid sequence with the NAD-dependent malate dehydrogenases (EC 1.1.1.37) from porcine cytoplasm (cMDH) (4, 5) and from a thermophilic bacterium *Thermus flavus* (tMDH) (6). This observation suggests that these MDHs share similar three-dimensional structures and that their coenzyme specificities are determined by a relatively limited number of amino acid residues. Particularly these amino acids must function in recognizing the presence or absence of a phosphate group at 2'-position of the adenine ribose ring in the nicotinamide nucleotide coenzymes. Crystallographic analysis of a cMDH·NAD complex at 2.5 Å resolution (7) revealed the presence of the typical $\beta\alpha\beta\beta$ dinucleotide-binding fold (8) and the 2'-hydroxyl group of NAD being hydrogen-bonded to the carboxyl group of Asp-41

located in a loop between β -strand B and α -helix C of this fold (Fig. 1). Several residues in this β B- α C loop, from Asp-41 to Gly-47, seem to be pointed toward the 2'-group of the cofactor and might be capable of participating in a putative 2'-phosphate-binding site. The sequence of the heptapeptide forming this loop in tMDH (Glu-41 \rightarrow Lys-47) shows limited similarity, two out of seven amino acids are identical to that of NAD-specific cMDH. However, neither tMDH nor cMDH has any sequence identity to that of the NADP-specific chMDHs in this loop (Fig. 2), suggesting that the amino acid sequence in this region might serve a principal role in determining the coenzyme specificity. To test this hypothesis, we constructed mutants in which the amino acids in this loop of tMDH were replaced by those in the corresponding region of chMDH and analyzed the kinetic properties of the altered enzyme.

MATERIALS AND METHODS

Construction and Expression of the Mutated Gene in *Escherichia coli*—All restriction and modification enzymes were purchased from Takara Shuzo. *E. coli* JM105 ($\Delta(lac\ pro)\ thi\ rpsL\ endA\ sbcB25\ hsdR4\ F'\ traD36\ proAB\ lacI^q\ lacZ\ \Delta M15$) was used both for DNA manipulation and the expression of the mutated *mdh* gene from *T. flavus* AT-62. A plasmid pTM101 was constructed by ligating 1.2-kilobase *Hind*III-*Sall* fragment from pTA2 (9) and pUC19 digested with the same enzymes for the efficient expression of the *mdh* gene. The mutation was introduced into the *mdh* gene by Kunkel's method (10). A 51-mer synthetic oligonucleotide (5'-CACGCCCTCCAGGGCCTGGAAGCTTCGCTCGGACCCAAAAGCTGGAGGAT-3') was used to replace the amino acid sequence from position 41–47 of tMDH, Glu-Ile-Pro-Gln-Ala-Met-Lys, by that of the corresponding portion of chMDH, Gly-Ser-Glu-Arg-Ser-Phe-Gln. The mutant was designated as EX7. A 28-mer synthetic oligonucleotide (5'-CTTCA TGGACTGGGGGATCCCAAAGC-3') was used as a mutagenic primer for the construction of the mutant enzyme having the Glu-41 \rightarrow Gly, Ile-42 \rightarrow Ser, and Ala-45 \rightarrow Ser exchanges; the mutant was named EX3. The mutated genes were expressed in *E. coli* JM105 under the control of the *lac* promoter on pUC19 by induction with 1 mM isopropyl- β -D-thiogalactopyranoside. The mutant tMDHs were purified, yielding a single band on SDS-polyacrylamide gel electrophoresis according to the methods reported previously (6).

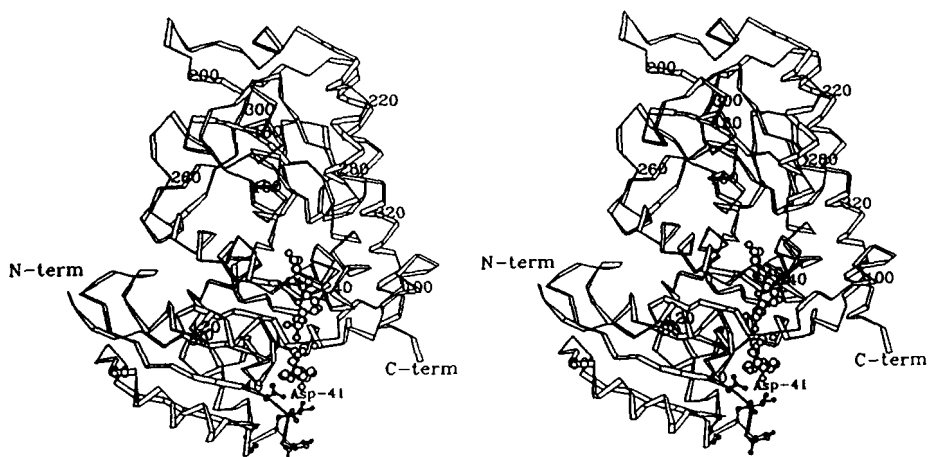
Steady-state Kinetic Analyses—Several series of steady-state kinetic analyses were carried out by measuring the decrease in absorbance at 340 nm in reaction mixtures containing 2–20 nM of the purified enzymes in 33 mM potassium phosphate buffer, pH 7.0, at 30 °C. In order to determine K_m for NAD(P)H, the concentrations of the coenzymes were varied in the range of 2–100 μ M employing a fixed oxaloacetate concentration (167 μ M) of in most of the experiments. However, 2 mM of oxaloacetate was used to determine K_m for NADPH of the wild-type enzyme, since no substrate inhibition occurred in these conditions as revealed in this work. In order to determine K_m for oxaloacetate, measurements were carried out by varying the oxaloacetate concentration (2–500 μ M) while keeping the NAD(P)H concentration fixed at 250 μ M. The kinetic constants for the EX3 mutant with NADH as a coenzyme were determined with varying concentrations of both oxaloacetate and NADH. Data were analyzed with the SUBIN, HYPER, and SEQUEN programs (11).

* This work was supported by a grant-in-aid from the Ministry of Education, Science, and Culture of Japan. The costs of publication of this article were defrayed in part by the payment of page charges. This article must therefore be hereby marked "advertisement" in accordance with 18 U.S.C. Section 1734 solely to indicate this fact.

‡ To whom correspondence should be addressed: Dept. of Agricultural Chemistry, Faculty of Agriculture, The University of Tokyo, Yayoi 1-1-1, Bunkyo-ku, Tokyo 113, Japan. Tel.: 3-3812-2111 (ext. 5126); Fax: 3-3812-0544.

¹ The abbreviations used are: chMDH, cMDH, and tMDH, malate dehydrogenase from chloroplasts, porcine cytoplasm, and thermophilic bacterium *Thermus flavus*, respectively.

FIG. 1. Stereo diagram of one subunit of cytoplasmic malate dehydrogenase. The stereo diagram shows a C α model of one cMDH subunit, drawn as a ribbon model. The bound NAD is drawn as a ball and stick model. The location in cMDH of the seven residues that in tMDH have been replaced in the EX7 mutant are shown as the smaller ball and stick model (see the text for additional detail). The residue numbers of every 20th amino acid are marked, and the location of the hydroxyl- and carboxyl-terminal ends are indicated.



| | 30 | 40 | 50 | 60 |
|-----------|-----------------------------------|----|-----------|----|
| chMDH(SV) | GQDQPIALKKLLGSSERSFQALEGVAMELEDSL | | | |
| | * * * * * | | * * * * * | |
| chMDH(ZM) | GQDQPIALKKLLGSSERSFQALEGVAMELEASL | | | |
| | * * * * * | | * * * * * | |
| tMDH | GKDQPVIILQLLEIPQAMKALEGVVMELEDC | | | |
| | * * * * * | | * * * * * | |
| cMDH | GKDQPIILVLLDITPMMLVLDGVLMELEQDC | | | |
| | | | | |
| | βB | | αC | |

FIG. 2. Alignment of the amino acid sequences in the region between β -strand B and α -helix C. chMDH(SV), chMDH(ZM), tMDH, and cMDH represent MDHs from *Sorghum vulgare* chloroplasts, *Zea mays* chloroplasts, *T. flavus*, and porcine heart cytoplasm, respectively. The amino acid residues identical to those of tMDH are indicated by asterisks while similar amino acids are also marked by dots. The residues in the β B- α C loop are boxed and the location of β -strand B and α -helix C are marked below the sequences. The amino acid sequence numbers above the sequences are those for cMDH.

The k_{cat} values thus obtained by modulating the concentrations of NAD(P)H and oxaloacetate, respectively, were nearly identical and the average values were used for calculation of the overall reaction efficiency defined as $k_{cat}/(K_m \text{ for oxaloacetate} \times K_m \text{ for NAD(P)H})$ (12). According to the ordered BiBi reaction mechanism of this malate dehydrogenase with two substrates, NAD(P)H (A) and oxaloacetate (B), formation of the ternary complex $E \cdot A \cdot B$ can be defined as $E \times A \times B / (K_m \text{ for A} \times K_m \text{ for B})$. By assuming transition state of the ternary complex as a rate-limiting step, overall reaction velocity can be expressed as $k_{cat} / (K_m \text{ for A} \times K_m \text{ for B}) \times E \times A \times B$, in which the overall catalytic efficiency defined here stands for the velocity constant at very low concentrations of the two substrates. k_{cat} for the wild-type enzyme (259.2 s^{-1} in Table I) obtained by varying the NADH concentration at a fixed oxaloacetate concentration ($167 \mu\text{M}$) might be underestimated due to substrate inhibition. Therefore, the overall catalytic efficiency of the wild-type enzyme for NADH was calculated by using a k_{cat} value (308.1 s^{-1}) obtained by variations in the oxaloacetate concentration.

Computer Graphic Manipulation—Model construction and analysis was conducted on a Silicon Graphics 4D IRIS workstation using the program TURBO (13). The crystal structure of the binary cMDH·NAD complex (7) was used as the starting template for modeling of the NADP binding site. The bound NAD coenzyme was converted into NADP by adding a phosphate group to the 2-hydroxyl group of the adenine ribose. Both the position and conformation of the modified NAD was left unchanged except for positioning of the added phosphate by rotation about the adenine ribose C2'-O2' bond. Residues 41–47 in the β B- α C loop in cMDH was replaced with the corresponding residues in chMDH, see Fig. 2. The polypeptide backbone was left unchanged, and side chains were adjusted by rotation about torsional bonds in order to minimize unfavorable nonbonded interactions with other protein atoms and with the NADP moiety.

RESULTS

Molecular Modeling—The high degree of amino acid sequence identity between cMDH and tMDH, 54%, suggests that these two forms of MDH have three-dimensional structures that closely resembles each other. Support for this comes from a model building exercise which demonstrated that the amino acid sequence of tMDH (6) could be incorporated into the cMDH crystal structure (7) without any major obstacles.² Difficulties were encountered only at position 41. In cMDH this residue is an aspartic acid and its carboxyl group interacts with the 2'- and 3'-hydroxyl groups in the adenine ribose. In all NAD dependent dehydrogenases of known structure a conserved aspartic acid is found in this position (8, 14). The only known exception is tMDH where residue 41 is a glutamate rather than an aspartate. However, the molecular modeling analysis suggests that despite the additional methyl group in glutamic acid Asp-41 can be replaced with a glutamate while maintaining the carboxyl group to hydroxyl group interactions. Comparisons of the chMDH amino acid sequences with those of cMDH and tMDH (Fig. 2) show that the structure of chMDH, at least in the vicinity of residue 41, closely resembles those of cMDH and tMDH. The replacement of residues 41–47 in cMDH with the corresponding ones in chMDH could be performed without requiring any adjustment in main chain conformation nor in the conformation in other parts of the subunit structure. Phe-46 (chMDH) can be positioned in the same hydrophobic pocket occupied by Met-46 in cMDH, and Ser-45 may be oriented to make a hydrogen bond to the carbonyl oxygen of residue 42 as shown in Fig. 3. The other side chains in the β B- α C loop are likely to point toward the external solvent. NADP differ from NAD by the presence of an additional phosphate at the 2'-hydroxyl groups in the adenine ribose. Analysis of the binary cMDH·NAD complex and of the putative cMDH·NADP complex showed that charge repulsion as well as steric crowding between the carboxyl group at position 41 and the NADP 2'-phosphate group should result in a decrease in affinity for NADPH. In addition, Ile-42 and Met-45 in cMDH, corresponding to Ile-42 and Ala-45 in tMDH, respectively, extend their hydrophobic side chains toward the 2'-hydroxyl group of NAD, which may prevent the 2'-phosphate group from being accepted at this position. In the mutant EX7, substituted according to the sequence of chMDH, residues 41, 42, and 45 are replaced by the smaller Gly, Ser, and Ser, respectively, permitting the NADP to be more readily accepted. The 2'-phosphate group is located in the space vacated by the side chain of residue 41.

² J. J. Birktoft, unpublished results.

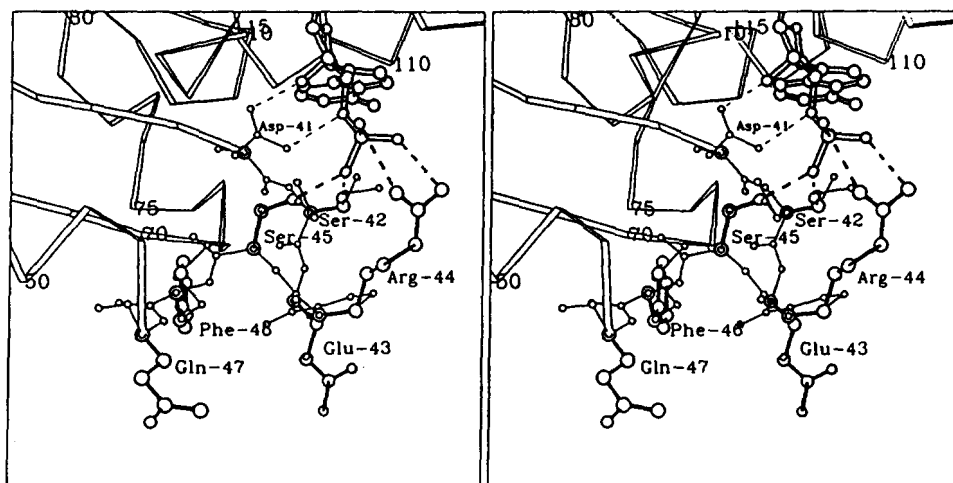


FIG. 3. Stereo diagram of the putative binding site in the EX7 mutant for the 2'-phosphate group of NADP. In this close-up view parts of the $C\alpha$ model of one cMDH subunit is shown as a ribbon model. The main chain and side chain atoms of cMDH residues 41-47 are shown as the smallest ball and stick models. The side chains of the seven residues replaced in tMDH are shown as larger ball and stick models with solid bonds. The positioning of the EX7 side chains are described in detail in the text. The bound NADP, in the same orientation as NAD in cMDH, is drawn as the largest ball and stick model, with hollow bonds. The stippled lines indicate possible hydrogen bonds between the EX7 side chains and the putatively positioned 2'-phosphate group. The residue numbers of every 5th $C\alpha$ in cMDH are marked, as are the residue names and numbers of EX7 residues 42-47. Residue 41 is in cMDH aspartate and is marked with a smaller label. This residue is in tMDH glutamate and in EX7 glycine.

TABLE I
Kinetic parameters of native and mutant tMDHs

| Enzymes and coenzymes | K_m | | | k_{cat} s^{-1} | k_{cat}/K_m $\mu M^{-1} s^{-1}$ |
|-----------------------|---------------|--------------|------------------|-----------------------|--------------------------------------|
| | For NADH | For NADPH | For oxaloacetate | | |
| Native | 3.05 ± 0.44 | 42.13 ± 4.26 | 2.38 ± 0.30 | 259.2 ± 10.8 | 85.0 |
| | | | 477.14 ± 22.46 | 308.1 ± 10.1 | 129.4 |
| NADPH | | | 164.4 ± 8.0 | 170.7 ± 5.0 | 3.9 |
| | | | 170.7 ± 5.0 | 170.7 ± 5.0 | 0.4 |
| EX7 | 82.69 ± 8.40 | 5.28 ± 0.56 | 16.80 ± 1.62 | 97.5 ± 4.6 | 1.2 |
| | | | 3.08 ± 0.34 | 100.2 ± 3.2 | 6.0 |
| NADPH | | | 152.2 ± 5.0 | 151.0 ± 3.3 | 28.8 |
| | | | 151.0 ± 3.3 | 151.0 ± 3.3 | 49.0 |
| EX3 | 51.19 ± 14.63 | 50.94 ± 6.22 | 487.98 ± 117.16 | 348.4 ± 60.5 | 6.8 |
| | | | 7.91 ± 0.34 | 348.4 ± 60.5 | 0.7 |
| NADPH | | | 347.9 ± 2.9 | 347.9 ± 2.9 | 6.8 |
| | | | 388.4 ± 18.4 | 388.4 ± 18.4 | 49.1 |

Irrespective of the conformation around the adenine ribose C2'-O2' bond the phosphate group appears to be pointed toward the solvent, and at least one of the phosphate oxygens would be in solvent contact. The side chain of Arg-44 is pointed to interact with the phosphate group, with the guanidinium group providing a neutralizing counter charge as shown in Fig. 3.

EX7 Mutation—The steady-state kinetic parameters of the wild-type tMDH and the mutant EX7, possessing the replaced loop sequence identical to that of cMDH, were determined by using NADH and NADPH as coenzymes, respectively. As shown in Table I, the mutation resulted in a markedly increased K_m for NADH; by a factor of 27 compared with wild-type tMDH, while K_m for NADPH was reduced by a factor of 8. In contrast the k_{cat} values were essentially unaffected by the mutation. The mutant enzyme retained a reasonably high turnover number in the presence of NADPH, which was nearly the half of that of the wild-type enzyme in the presence

of NADH. Taking k_{cat}/K_m as a simple measure of catalytic efficiency, the mutation was judged to cause a 7-fold improvement with NADPH as cofactor and a 71-fold decrease in efficiency with NADH as cofactor. The consequence of the replacement of the seven βB - αC loop amino acids was that tMDH was changed from being a NAD-specific dehydrogenase into a NADP-specific one.

EX3 Mutation—In order to test whether substitution of only a limited number of the amino acids in the βB - αC loop were sufficient to cause a conversion of coenzyme specificity the tMDH EX3 mutant was constructed with the exchanges of Glu-41 → Gly, Ile-42 → Ser, and Ala-45 → Ser. In the reaction with NADH as a coenzyme, the EX3 mutations resulted in increases of the K_m values for NADH and oxaloacetate by factors of 17 and 205, respectively (Table I). However, in the reaction with NADPH as a coenzyme, the K_m value for oxaloacetate was decreased 60-fold, while the K_m value for NADPH was unchanged. Consequently, taking $k_{cat}/$

K_m value as a measure, the replacement of residues 41, 42, and 45 mutation led to a 12-fold decrease in efficiency with NADH, and an approximately 2-fold improvement in efficiency with NADPH.

Evaluation of the Mutations—When the reactions with wild-type tMDH were carried out with NADH as a coenzyme, the K_m value for oxaloacetate was quite low, but very large with NADPH as a cofactor. This suggests that the binding of oxaloacetate to wild-type tMDH is noticeably facilitated by binding of NADH but inhibited by NADPH. Both the mutations, EX7 and EX3, caused drastic decreases, 150- and 60-fold, respectively, in the K_m value for oxaloacetate with NADPH as a cofactor, while the K_m value with NADH was increased significantly. These results indicate that these mutations influence markedly not only the K_m for NAD(P)H, but also the K_m for oxaloacetate. Although a corresponding large change in K_m for the substrate was observed with mutations at the corresponding site of lactate dehydrogenase from *Bacillus stearothermophilus* (12), it was proposed that the effect of the mutation on the efficiency for NADH or NADPH could be evaluated by incorporating the K_m for the substrate. This parameter is called the overall catalytic efficiency, which is defined by the equation $k_{cat}/(K_m,oxaloacetate \times K_m,NAD(P)H)$. As shown in Table II, the EX7 mutation resulted in a 1118-fold improvement in the overall catalytic efficiency for NADPH, while the efficiency for NADH decreased 600-fold. The ratio of these two contrasting shifts is 6.7×10^5 , indicating an almost complete conversion of the coenzyme specificity. On the other hand, the EX3 mutation resulting from the replacement of 3 amino acids caused a 110-fold improvement in the overall catalytic efficiency for NADPH, whereas it led to a 3050-fold decrease in the efficiency for NADH. The ratio of these shifts toward NADPH was 3.4×10^6 , which differ just 2-fold from the value for EX7. These results suggest that the alteration of the coenzyme specificity induced by EX7 mutation with 7 amino acid substitutions was mainly caused by the 3 amino acid replacements in EX3.

NADH-dependent Substrate Inhibition of tMDH—We had previously observed that wild-type tMDH was strongly inhibited by excess concentrations of oxaloacetate in the presence of NADH as a coenzyme (6). On the other hand, as shown in Fig. 4A, the enzyme was no longer subject to substrate inhibition when NADPH was used as a coenzyme. When the similar analysis was performed with the mutant enzyme EX7, the substrate inhibition was again observed in the presence

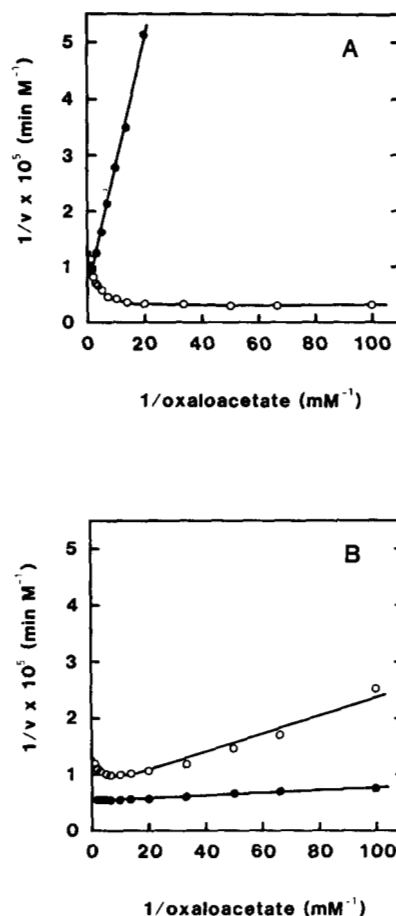


FIG. 4. Double-reciprocal plots of the wild-type and EX7 mutant enzymes. A, wild-type tMDH; B, EX7-tMDH, with NADH (○) or NADPH (●) as a coenzyme.

of NADH but not NADPH (Fig. 4B). Taken together these results demonstrate that the substrate inhibition in tMDH seems to depend on the presence of NADH as a coenzyme.

DISCUSSION

Site-directed mutagenesis have been attempted to alter the coenzyme specificity in other dehydrogenases. The residues located in the β B- α C loop were in all instances the target for the replacements. In the case of lactate dehydrogenase from *B. stearothermophilus*, Asp-53 which corresponds to Asp-41 in cMDH and Glu-41 in tMDH was replaced by a serine (12). The mutation caused a decrease in the overall catalytic efficiency with NADH as cofactor but had almost no effect on the efficiency with NADPH as cofactor. As a consequence, the mutants still retained the original preference for NAD over NADP; *i.e.* the coenzyme specificity was not fully converted. The most extensive alteration of the coenzyme specificity in a nicotinamide adenine-dependent oxidoreductase was achieved with the NADP-dependent glutathione reductase, in which cumulative replacement of the residues in not only the loop between β -strand B and α -helix C but also in an adjacent α -helix were carried out (15). These mutations caused the ratio of efficiencies (k_{cat}/K_m) for NADPH and NADH to shift 18,000-fold in favor of NADH. However, even for the most altered mutant the k_{cat}/K_m with NADH as cofactor was only 1/30 of that for the wild-type enzyme with NADPH as cofactor. In the study reported here, seven amino acid residues forming the β B- α C loop were chosen as the targets for changing the coenzyme specificity of tMDH. As reflected in both K_m and k_{cat} values an almost complete

TABLE II

| Overall catalytic efficiencies of the native and mutant tMDHs | | |
|---|---|-------------------------|
| Coenzymes and enzymes | k_{cat} | |
| | $(K_m^{OA}) \times (K_m^{NADH})$ | $M^{-2} \cdot sec^{-1}$ |
| NADH | | |
| Native | $\frac{308.1}{(2.38 \times 10^{-6}) \times (3.05 \times 10^{-6})}$ | $= 4.24 \times 10^{13}$ |
| EX7 | $\frac{98.9}{(16.8 \times 10^{-6}) \times (82.69 \times 10^{-6})}$ | $= 7.09 \times 10^{10}$ |
| EX3 | $\frac{348.4}{(487.98 \times 10^{-6}) \times (51.19 \times 10^{-6})}$ | $= 1.39 \times 10^{10}$ |
| NADPH | | |
| Native | $\frac{167.6}{(477.14 \times 10^{-6}) \times (42.13 \times 10^{-6})}$ | $= 8.34 \times 10^9$ |
| EX7 | $\frac{151.6}{(3.08 \times 10^{-6}) \times (5.28 \times 10^{-6})}$ | $= 9.32 \times 10^{12}$ |
| EX3 | $\frac{368.2}{(7.91 \times 10^{-6}) \times (50.94 \times 10^{-6})}$ | $= 9.17 \times 10^{11}$ |

conversion of the coenzyme specificity was achieved by changing just the 7 amino acids in the β B- α C loop region of tMDH. Furthermore, the alteration of the coenzyme specificity was caused primarily by the replacements of only 3 amino acid residues of the loop. However, it is noteworthy that in the EX3 mutation the K_m values were increased not only for NADH but also for oxaloacetate with NADH. This was accompanied with a decrease in the K_m value for oxaloacetate in the presence of NADPH, but not by a decrease of the K_m value for NADPH, suggesting that some of the additional four substitutions in EX7 participate in decreasing the K_m value for NADPH. We assume that the most likely candidate for this function in EX7 is the Gln-44 \rightarrow Arg substitution since the positive charge of the arginine side chain may facilitate and stabilize the binding of 2'-phosphate of the adenine ribose. This suggestion is supported by the molecular modeling of EX7. The guanidinium group Arg-44 can by simple side chain rotation be brought into close proximity to the 2'-phosphate adenine ribose moiety as shown in Fig. 3.

Our previous work with a series of the mutant tMDHs of Thr-189, located close to the catalytic residue His-186, revealed that desensitization of the enzyme toward substrate inhibition was achieved by mutations that increased the K_m for oxaloacetate (9). However, this rule does not fit with the present results obtained with the EX7 and EX3 mutants in the presence of NADPH, because desensitizations were observed with NADPH which showed reduced K_m for oxaloacetate. This NADH-dependent inhibition by oxaloacetate may suggest that some specific interaction between the substrate and NADH, that differs from the productive substrate-coenzyme complex, might be responsible for the substrate inhibition. A similar implication was also suggested by the marked effect of NADH to decrease K_m for oxaloacetate in the wild-type enzyme. According to the three-dimensional structure of the binary cMDH·NAD complex, however, the 2'-hydroxyl group of NAD is pointed to the β B- α C loop which is located quite distant from the oxaloacetate-binding site (7). In lactate dehydrogenase from *B. stearothermophilus*, the binding of NADH and pyruvate was reported to cause a marked rearrangement of the flexible loop between β -strand D and α -helix D, which contained an arginine residue hydrogen-bonded to the reactive carbonyl of the substrate and to the

imidazole ring of the catalytic histidine (16). Therefore, we may speculate that a specific local conformational change induced by the binding of NADH or NADPH is responsible for relatively large modulation in behavior of tMDH toward oxaloacetate. High quality crystals of a tMDH·Thr-189 \rightarrow Ile·NADH complex has recently been obtained (17), and the refined high resolution structure of tMDH should be available in the near future. Furthermore, we have also succeeded in crystallizing not only EX7·NAD complex but also EX7·NADP complex.³ The crystallographic analyses of the native and the altered tMDHs should reveal the functional contribution of each of the residues in the loop region toward the coenzyme specificity.

Acknowledgment—We are grateful to Dr. H. Sakai (Department of Agricultural Chemistry, The University of Tokyo) for kind advice on the kinetics in this study.

REFERENCES

1. Fickenscher, K., Scheibe, R., and Marcus, F. (1987) *Eur. J. Biochem.* **168**, 653–658
2. Metzler, M. C., Rothermel, B. A., and Nelson, T. (1989) *Plant Mol. Biol.* **12**, 713–722
3. Cretin, C., Luchetta, P., Joly, C., Decottignies, P., Lepiniec, L., Gadal, P., Sallantin, M., Huet, J.-C., and Pernollet, J.-C. (1990) *Eur. J. Biochem.* **192**, 299–303
4. Birktoft, J. J., Bradshaw, R. A., and Banaszak, L. J. (1987) *Biochemistry* **26**, 2722–2734
5. Joh, T., Takeshima, H., Tsuzuki, T., Setoyama, C., Shimada, K., Tanase, S., Kuramitsu, S., Kagamiyama, H., and Morino, Y. (1987) *J. Biol. Chem.* **262**, 15127–15131
6. Nishiyama, M., Matsubara, N., Yamamoto, K., Iijima, S., Uozumi, T., and Beppu, T. (1986) *J. Biol. Chem.* **261**, 14178–14183
7. Birktoft, J. J., Rhodes, G., and Banaszak, L. J. (1989) *Biochemistry* **28**, 6065–6081
8. Rossmann, M. G., Liljas, A., Brändén, C. I., and Banaszak, L. J. (1975) in *The Enzymes*, (Boyer, P. D., ed) 3rd Ed., Vol. 11, pp. 61–102, Academic Press, New York
9. Nishiyama, M., Shimada, K., Horinouchi, S., and Beppu, T. (1991) *J. Biol. Chem.* **266**, 14294–14299
10. Kunkel, T. A. (1985) *Proc. Natl. Acad. Sci. U. S. A.* **82**, 488–492
11. Cleland, W. W. (1979) *Methods Enzymol.* **63**, 103–138
12. Feeney, R., Clarke, A. R., and Holbrook, J. (1990) *Biochem. Biophys. Res. Commun.* **166**, 667–672
13. Roussel, A., and Cambillau, C. (1991) *Silicon Graphics Directory*, p. 86, Silicon Graphics, Mountain View, CA
14. Birktoft, J. J., and Banaszak, L. J. (1984) in *Pept. Protein Rev.* **4**, 1–46
15. Scrutton, N. S., Berry, A., and Perham, R. N. (1990) *Nature* **343**, 38–43
16. Clarke, A. R., Wigley, D. B., Chia, W. N., Barstow, D., Atkinson, T., and Holbrook, J. J. (1986) *Nature* **324**, 699–702
17. Kelly, C. A., Sarfaty, S., Nishiyama, M., Beppu, T., and Birktoft, J. J. (1991) *J. Mol. Biol.* **221**, 383–385

³ C. A. Kelly, M. Nishiyama, M. Kukimoto, T. Beppu, and J. J. Birktoft, unpublished data.